Atmos. Chem. Phys. Discuss., 15, 9077–9106, 2015
www.atmos-chem-phys-discuss.net/15/9077/2015/
doi:10.5194/acpd-15-9077-2015

Atmospheric Chemistry and Physics
Discussions
Open Access

PLAM – a meteorological pollution index for air quality and its applications in fog-haze forecasts in north China

Y. Yang[1], J. Wang[1], S. Gong[1], X. Zhang[1], H. Wang[1], Y. Wang[1], J. Wang[2], D. Li[3], and J. Guo[1]

[1]Institute of Atmospheric Composition/Key Laboratory of Atmospheric Chemistry of China Meteorological Administration (CMA), Chinese Academy of Meteorological Sciences (CAMS), Beijing 100081, China
[2]National Meteorological Information Centre, CMA, Beijing 100081, China
[3]National Climate Centre, CMA, Beijing 100081, China

Received: 11 December 2014 – Accepted: 19 January 2015 – Published: 25 March 2015

Correspondence to: S. Gong (sunling@cams.cma.gov.cn) and J. Wang (wjz@cams.cma.gov.cn)

Published by Copernicus Publications on behalf of the European Geosciences Union.

Abstract

Using surface meteorological observation and high resolution emission data, this paper discusses the application of PLAM/h Index (Parameter Linking Air-quality to Meteorological conditions/haze) in the prediction of large-scale low visibility and fog-haze events. Based on the two-dimensional probability density function diagnosis model for emissions, the study extends the diagnosis and prediction of the meteorological pollution index PLAM to the regional visibility fog-haze intensity. The results show that combining the influence of regular meteorological conditions and emission factors together in the PLAM/h parameterization scheme is very effective in improving the diagnostic identification ability of the fog-haze weather in North China. The correlation coefficients for four seasons (spring, summer, autumn and winter) between PLAM/h and visibility observation are 0.76, 0.80, 0.96 and 0.86 respectively and all their significance levels exceed 0.001, showing the ability of PLAM/h to predict the seasonal changes and differences of fog-haze weather in the North China region. The high-value correlation zones are respectively located in Jing-Jin-Ji (Beijing, Tianjin, Hebei), Bohai Bay rim and the southern Hebei-northern Henan, indicating that the PLAM/h index has relations with the distribution of frequent heavy fog-haze weather in North China and the distribution of emission high-value zone. Comparatively analyzing the heavy fog-haze events and large-scale fine weather processes in winter and summer, it is found that PLAM/h index 24 h forecast is highly correlated to the visibility observation. Therefore, PLAM/h index has better capability of doing identification, analysis and forecasting.

1 Introduction

Compared with 1980s, fog-haze pollution events have increased significantly in the recent decade in the Beijing and North China region. Meteorological condition is one of the important elements that impact the local aerosol accumulation and contributes to the frequent appearance of low visibility weather (Wang et al., 2010, 2002). The synthetic impact analysis on the pollution-related atmospheric dynamic, thermodynamic and chemical processes as well as the fog-haze prediction study has drawn widely attentions. Long-term observations have pointed out that in the last 30 years fog-haze phenomenon in the central and eastern part of China has become more and more serious due to anthropogenic emissions. Under some meteorological conditions, aerosol particles in the atmosphere can be activated into cloud condensation nuclei (CCN), participating in the formation of clouds and fog, which means that modern fog-haze have involved lots of polluted aerosol particles (e.g. $PM_{2.5}$). To reduce the impact of the weather disaster of fog-haze, special attentions need to be given to atmospheric aerosol pollution (Zhang et al., 2013) The 3-dimensional numerical model has been progressed in different degrees in the meteorological services of the global air quality predictions (McKeen, 2007; Moran, 2009; Zhang, 2009). Chemical forecasting model study and prediction usually faces the problems of timely emission data all over the world, therefore limits the ability to improve the forecasting accuracy. In recent years, through analyzing the observation data of atmospheric aerosol particulate matter (PM) and the physical connection of sensitive meteorological parameters, the establishment of air quality parameterized diagnostic predicting method has being developed. Research results revealed that the air quality meteorological index PLAM (Parameter linking Air-quality to Meteorological conditions) can achieve reasonable results when it was applied in the prediction of the air quality in Beijing during the 2008 Beijing Olympic Games. The identification and prediction researches of meteorological condition PLAM index to air quality have achieved progresses at home and abroad in recent years (Zhang et al., 2009; Honoré et al., 2008; Li et al., 2011; Kassomenos et al., 2008; Yang et al., 2009; Wang et al., 2013). Researches indicate that the contribution of meteorological condition PLAM index from emissions is of great importance as they have remarkable impacts on the regional distribution of air qualities in different areas. However, there are very limited researches on emission contribution to the air quality meteorological index, including its quantitative expression, physical mechanism and diagnostic prediction. This is especially critical in establishing the relations and mechanism of large-scale high-value $PM_{2.5}$ and low visibility weather.

On the basis of parameterized meteorological condition principle method, this paper is to discuss the mutual impact of emission and meteorological condition, and study the structure and function of meteorological conditions PLAM index in quantitatively identifying, diagnosing and forecasting large scope of fog-haze weather.

2 Data and methods

This paper uses the near real-time (NRT) operational data, including surface observation data, from which the elements related to meteorological condition impact are extracted such as atmospheric temperature, difference of temperature and dew point, clouds, weather phenomenon, air pressure, wind direction and speed and visibility, and high-level sounding data as well as the data from atmospheric component observing system stations. The multi-source element data including high resolution emission data were analyzed to investigate the meteorological condition PLAM index identification method for forecasting wide-range low visibility and fog-haze.

2.1 Analysis on wet-equivalent potential temperature θ_e features of uniform air mass

Air quality and meteorological condition impacts are closely related. Usually different air mass structures can lead to significant difference of meteorological conditions. Studies pointed out that, aiming at the impact on air quality, it is very important to analyze and distinguish what kind of air mass controls and affects the local area, identify the differences of atmospheric aerosol features of the air masses in different types including maritime air mass, continental air mass or polar air mass etc., and consider the identification of stagnant air mass. The property of wet-equivalent potential temperature θ_e can be used to distinguish the types of air masses, because θ_e includes dry and wet adiabatic processes, lifting condensation and sinking and other dynamic and thermodynamic processes in atmosphere, having the property of conserving and being able to be tracked and identified. The equation of wet-equivalent potential temperature is:

$$\theta_e = \theta \exp\left[\left(\frac{L_w}{C_p T}\right)\right] \tag{1}$$

where: θ is potential temperature:

$$\theta = T\left[\left(\frac{1000}{P}\right)^{\frac{R_d}{C_p}}\right] \tag{2}$$

the unit of θ and θ_e is K. w, C_p, L, R_d, P and T are mixing ratio, constant-pressure specific heat ($C_p = 1.005\,\mathrm{J\,g^{-1}\,degree^{-1}}$), latent heat of condensation of water vapor ($L = 2500.6\,\mathrm{J\,g^{-1}}$), gas constant ($R_d = 2.87 \times 10^{-1}\,\mathrm{J\,g^{-1}\,degree^{-1}}$), air pressure and temperature, respectively.

2.2 Parameterized method of diagnosing and forecasting atmospheric process

The interactions and mutual effects of atmospheric micro-physical process and larege-scale process as well as the different scales of process are very complicated in the transient of cloud and fog physical process as well as the atmospheric pollution process. The meaning and main idea of the parameterized method is to connect the non-linear relationship that is difficult to describe in the processes of different scales with a parameterization sheme. Studies (Kuo, 1961, 1965, 1974) have shown that the micro-processes in cloud physics can be described in a parameterization scheme with the large-scale observations. Based on the Lagrangian method the variation of fluid particle group going with time can be followed, i.e, identifying the “stagnant and less changing” state of air masses. In the atmospheric particle movement, the individual change of wet-equivalent potential temperature (spatial–temporal total derivative) gets to a small value or zero, meaning little changes. Therefore, according to the identification of the "stagnant and less changing" property of wet-equivalent potential temperature of air masses, i.e., the basic physical process of $\mathrm{d}\theta_\mathrm{e}/\mathrm{d}t \approx 0$, the possible varying trend of air quality of the "stagnant and less changing" air masses can be diagnosed and predicted. The recently developed air quality diagnosis of parameterized meteorological conditions (Yang et al., 2009; Zhang et al., 2009; Wang et al., 2012) PLAM index is described as follows:

$$\mathrm{PLAM}_0 = \frac{\mathrm{d}\theta_\mathrm{e}}{\mathrm{d}t} \cong \theta_\mathrm{e}\frac{f_\mathrm{c}}{C_\mathrm{p}T} \tag{3}$$

θ_e is wet-equivalent potential temperature given out by Eq. (1). f_c is wet air condensation rate:

$$f_\mathrm{c} = f_\mathrm{cd} \Bigg/ \left[\left(1 + \frac{L}{C_\mathrm{p}}\frac{\partial q_\mathrm{s}}{\partial T}\right)_\mathrm{p}\right] \tag{4}$$

f_cd is dry air condensation rate:

$$f_\mathrm{cd} = \left[\left(\frac{\partial q_\mathrm{s}}{\partial P}\right)_T + \gamma_\mathrm{p}\left(\frac{\partial q_\mathrm{s}}{\partial T}\right)_\mathrm{p}\right] \tag{5}$$

γ_p is dry-adiabatic lapse rate:

$$\gamma_\mathrm{p} = \frac{R_\mathrm{d}}{C_\mathrm{p}} \times \frac{T}{P} \tag{6}$$

q_s is specific humidity. The meanings of other variables are the same as the above-mentioned.

The Eq. (3) shows that the parameterized method based on the spatial–temporal variation of wet-equivalent potential temperature of air masses has practical application prospect in analyzing, diagnosing and forecasting the changes of air quality. The objective of this paper is to further discuss the impact and identification of PLAM_0 index to aerosol pollution concentration accumulative increase and atmospheric fog-haze weather, and moreover study the possibility of using the parameterized method to improve the diagnosing and forecasting capability to large-scale disastrous fog-haze weather.

2.3 Contribution and impact of atmospheric emission on PLAM index

Considering the diagnosis and forecasting analysis of atmospheric fog-haze which is closely related to atmospheric aerosols (such as fine particle $\text{PM}_{2.5}$ etc.), it is very important to integrate the effect of the initial meteorological conditions PLAM_0 and emission contribution. In order to integrate the initial meteorological condition related to atmospheric pressure, temperature, humidity, condensation, etc. with the contribution of the pollutant emission factor p in the atmosphere, the identification parameter was expressed by Eq. (7) (Wang et al., 2012):

$$\text{PLAM\_haze} = \text{PLAM}_0 \times p \tag{7}$$

This factor p further expands the application of PLAM index and investigates the description of the function and impact of the index by emissions in the forming and developing process of regional wide-range fog-haze event, namely PLAM_haze (abbreviated as PLAM/h). Thus, analysis on the latest emission research results as of 2010 is introduced including industry, energy source, transportation, anthropogenic emission source combined $E_{\text{PM}_{2.5}}$ (Unit: $\text{t} \times 10$) (Fig. 1a). It is seen from Fig. 1a that the high-value zones from industry, energy source, transportation and anthropogenic emission source in the North China region involve (1) the central and southern part of Hebei (including Beijing and Tianjin), (2) the central and western part of Shandong, (3) the central part of Henan, (4) the eastern part of Hubei, (5) the Yangtze River delta and (6) the eastern part of Sichuan (the Chengdu Plain). All these high-value emission sources have significant impacts on the fog-haze weather in North China and cannot be underrated.

To quantify the impact of emission in PLAM index, the probability of its impact on the surrounding area satisfies the normal distribution, that is, by separating the impacts of meteorological condition and emission on the surrounding part, it is always isotropic and the impact probability of high emission center area is higher than that of the surrounding area. As a result, the emission impact satisfies the form of 2-dimensional probability distribution, and the integral probability density function that falls into the surrounding limited area x, y plane (s) is as follows (Wang et al., 1985; Neumann et al., 1978):

$$P'(s) = \iint_{\mathrm{s}} f(x,y)\mathrm{d}x\mathrm{d}y = 1 - \exp(-\gamma^2/2) \tag{8}$$

where γ is the standardized (normalized) grade of the emission source intensity in the concerned forecasting area, $\gamma \in (0,1)$, defined as $\gamma = (E - E_{\min})/(E_{\max} - E_{\min})$, where $E_{\max}$ and $E_{\min}$ are the maximum value and minimum value of the emission E in the specified season of the studied impact region (North China). In other words, the exponential growth rate with emission impact is $P = 1 + P'$. Then, the impact of emission on the increase value of fog-haze is taken into account, and the Eq. (3) can be formulated into:

$$\mathrm{PLAM/h} = \theta_{\mathrm{e}} \frac{f_{\mathrm{c}}}{C_{\mathrm{p}}T} \times p(\gamma) \tag{9}$$

3 Results and discussion

3.1 Analysis on PLAM index medium emission contribution features

Studies pointed out that emission does not change very much in certain fixed temporal scales (such as a month or a season) in the same area, but differs greatly in different places. To analyze the contribution of regional emission on the low visibility weather like fog-haze, the comparable standardized emission intensity (γ) in the regional and seasonal period was calculated based on the meteorological observation data in different places and different time periods. Figure 1a presents the distribution of high resolution emission lists. Figure 1b is the standardized distribution of emission list in the North China region based on Fig. 1a. From Fig. 1b, it can be seen that (1) Beijing, Tianjin and the central and southern part of Hebei, (2) the west of Shandong, (3) the central part of Henan, (4) the eastern part of Hubei, (5) the Yangtze river delta and (6) the east of Sichuan remain to be the significantly concentrated high emission regions, whose circular or oval-shaped distribution characteristics are clearly seen. Taking the rarely-seen large-range heavy fog-haze weather event over Beijing and the North China region on 26 February 2014 as an example, the difference by considering and ignoring the emission contribution in PLAM index is discussed. Figure 1c and d show the PLAM index distribution under the condition of considering and ignoring the emission in North China at 08:00 (UTC +8) 26 February 2014. It is seen from the figure that under the condition without considering the emission impact (Fig. 1c) the distribution centers of PLAM index are: Hebei, Beijing-Tianjin region in North China; southern Hebei, northern Henan; western Hubei and northern Sichuan. The PLAM indices are 120, 160, 160, and 80 (Fig. 1c) respectively. Figure 1d shows PLAM/h distribution with the emission impact. The above-mentioned four PLAM/h index high value zones are 180, 180, 180 and 160, respectively. The PLAM/h value increases along with the significant expansion of high-value (the green oval-shaped circle in the figure).

To further discuss the difference, Fig. 2 displays the correlation analysis of 24 h forecasting and visibility of PLAM/h index at 673 stations in North China on 26 February 2014. For the convenience to compare, the overlap of the correlation distributions of PLAM/h and visibility under the condition of including and excluding emission factors is given out. The considered emission in Fig. 2 is expressed by blue triangle while the ignored emission is marked with red circle–yellow filled circle. The correlation fitted lines are respectively marked by red solid line and black dashed line. It is seen from Fig. 2 that the reasonable correlation exists between PLAM/h and visibility on 26 February 2014 regardless of emission contributions. However, correlation coefficient (R^2) is increased from 0.3675 to 0.3887 when emissions are considered.

It is noted that in the low-value visibility range (Vis $<$ 10 km), the PLAM/h index value without emission impact shifts towards low-value zone clearly. Comparatively, the closer to the high-value zone of visibility, the more the two types of symbols tend to overlap, which suggests that, without emissions, the predictive value of PLAM/h index will be smaller and its correlation with visibility will be reduced, deviating the fitted low-value zone line.

In summary, the above analyses on the regional PLAM/h distribution (Fig. 1) and the correlation distribution of PLAM/h and visibility (Fig. 2) all indicate that with the combined impact of meteorological condition and emission factors, the description capability of PLAM/h index increases significantly with the index value expanding to the high-value zone; the PLAM/h index including the emission has obvious impact on improving the capability of diagnosing and identifying the heavy fog-haze weather.

3.2 Analysis on seasonal characteristics of PLAM/h index and visibility correlation

Figure 3 separately presents distribution of fog-haze weather in the typical heavy fog-haze process cases in four seasons, including the PLAM/h (Fig. 3a) and visibility (Fig. 3b) of the 14 April 2011 spring case, the PLAM/h (Fig. 3c) and visibility (Fig. 3d) of the 26 July 2008 summer case, the PLAM/h (Fig. 3e) and visibility (Fig. 3f) of the 30 October 2011 autumn case and the PLAM/h (Fig. 3g) and visibility (Fig. 3h) of the 7 January 2011 winter case.

In spring, the PLAM/h index low-value zone on 14 April 2011 is mainly in the North China region. 3/4 regional PLAM/h < 70 in the whole region. The meteorological condition is good for pollutants to diffuse. There is a weak PLAM/h relatively high-value zone across the central Henan, southern Hebei, Beijing-Tianjin and northern Hebei, which is PLAM/h ≥ 80. Besides, there is another high-value zone in the coastal parts of Bohai Sea, corresponding to the sea fog prone area in the southern part of North China. The PLAM/h high value matches with the low-value zone of visibility whist the large-range PLAM/h low-value zone goes with the high-value zone of visibility.

In Summer, the 08:00 (UTC +8) 26 August 2008 case shows that the North China region is a large-scale PLAM/h high-value zone, whose center distributes in north–south banding shape: (1) east of Taihang Mountains in Henan province to southern Hebei (PLAM/h value is 120 and the highest even gets to 200), (2) Beijing and central Hebei (PLAM/h value is 120–140), (3) the Jing-Jin-Tang (Beijing, Tianjin, Tangshan) region (PLAM/h value is high up to 120–240) and (4) the west-southern Shandong (PLAM/h value reaches 140–200) are four remarkable banding high value centers. Corresponding to the wide-range low visibility low value zones, the visibility in most parts is lower than 10 km, of which the visibility from Henan to southern Hebei is lower than 4 km. The Beijing-Tianjin region has the visibility of 4–8 km only. So, PLAM/h index has significant effect on diagnosing and identifying the summer fog-haze weather in North China.

North China usually has clear and refreshing autumn weather. But in recent years, heavy fog-haze weather events appear more and more frequently in autumn. To examine the identifying capability of PLAM/h index in the typical autumn heavy fog-haze case, we analyze the rarely seen heavy fog-haze pollution process that happened in North China on 30 October 2011. According to Fig. 3g and h, the high-value PLAM/h index in the fog-haze area in North China assumes in the north–south trend parallelized to the regional distribution of three large-scale bands (Fig. 3g) and PLAM/h > 200–240, of which the three high-value PLAM/h bands are parallel to the Taihang Mountains in North China, orderly arranged along the line of the boundary between Shanxi and

Hebei-southern Liaoning (dotted line in the figure) and being greatly consistent with the banding distribution of the fog-haze and low visibility areas in North China (Fig. 3h). The large scope of PLAM/h low-value zone, PLAM < 20–50, in the western and northern parts of North China agrees with the high-value visibility zone with Vis > 20 km. Therefore, PLAM index has the characteristics of weather-scale banding distribution similar to the distribution of weather systems.

One heavy fog-haze process rarely seen in history appeared in North China in the first-half month of January 2013. This is a typical winter heavy fog-haze case, whose PLAM/h index is significantly high, indicating the contribution of meteorological condition to the enhancement and persistence of this large-range fog-haze process is dominating. PLAM/h index high-value zone blankets the Beijing-Tianjin, the east to Taihang Mountains to the most part of North China which is to the south of Yanshan Mountains. The banding fog-haze weather area in the southwest-northeast trend extends eastward into the southern part of Liaoning. Corresponding to the southwest-northeast trend banding high-value zone of PLAM/h index (Fig. 3g), the visibility is the accordant banding low-value distribution area (Fig. 3h).

The seasonal results analysis of PLAM/h index shows its characteristics linkage with weather-scale system in each season. The weather-scale high-value PLAM/h zone agrees with the low-value visibility area, which indicates the regional distribution of PLAM/h index is indicative of diagnosing, identifying and forecasting the large-range fog-haze area in four seasons in North China.

Figure 4 reveals the correlation of PLAM/h index and visibility in different seasons which is calculated by Eq. (9) according to the 2009 daily observation data in Beijing. As the seasonal features related to aerosol pollution in North China are different from the seasonal features divided according to temperature elements, the selected representative stations are slightly different. For the analysis of this paper, the season from July to August is defined as rainy season or summer and from November to the next February is winter in North China. Spring and autumn are two transition seasons, taking March to June and September to October respectively. In Fig. 4a the chosen period of winter includes January–February and November–December of Beijing (BJ) and Zhengzhou (ZZ), there are totally 240 groups of observation record. In Fig. 4b there are totally 248 groups of observation records chosen for the summer July–August of Beijing (BJ), Zhengzhou (ZZ), Taiyuan (TY) and Jinan (JN). Figure 4c involves 122 groups of records from Beijing (BJ) for the season of spring March–June. Figure 4d contains 122 groups of observation records for the autumn September–October of Beijing (BJ) and Zhengzhou (ZZ). It is seen from the figures that:

1. The variation of air quality meteorological condition PLAM/h index is significantly correlated to the visibility observation (Vis) in Beijing and the correlation coefficients (R^2) are 0.8587 (winter), 0.8009 (summer), 0.7617 (spring) and 0.9552 (autumn), respectively, with all significance levels exceeding 0.001.
2. In winter (Fig. 4a), with the low-value meteorological condition index, when PLAM/h < 80, Vis > 25 km; when high value of PLAM/h gets up to 150–350, the observed visibility trend gets worse with Vis < 10 km. Different from winter, during the low-value meteorological condition index in summer, when PLAM < 100, Vis < 10 km; when the PLAM high value rises to 150, the observed visibility becomes worse and Vis < 5 km (Fig. 4b). This means that PLAM/h has significant capability to describe optimal or inferior visibility, and, moreover, its seasonal difference is great. This finding is consistent with the climate observation result that the aerosol concentration high value in summer appears at the same pace with low visibility (Wang, 2006).
3. Figure 4 shows that the correlations in the two transition seasons are noticeably different. The correlation features in spring are similar to those in summer while the autumn features are like winter's. But during the transition seasons, spring and autumn, the threshold value deduced from the diagnosis of PLAM/h to heavy fog-haze pollution is lower, that is, when the meteorological condition index PLAM/h gets to 150, visibility is with very low value, even Vis < 5 km.

In summary, the above analyses indicate that PLAM/h is capable to describe the changes of visibility, and also capable of distinguishing the seasonal differences very well. The seasonal threshold difference resulting from the diagnosis of PLAM/h to heavy fog-haze pollution is indicative of quantitatively identifying and diagnosing the appearance of fog-haze pollution.

3.3 PLAM index and related features of visibility area

Figure 5 shows the regional correlation between PLAM/h index and visibility which is obtained by calculating the 1006 groups of observation samples collected from January 2009 to December 2012. The regional distribution of the correlation with significance level exceeding 0.001 is also shown. The figure indicates that most part of North China is the high-value zone > 80 %, of which one high-value zone is located in Shanxi, most Hebei, southern Hebei and Northern Hubei, being likely related to the favorable meteorological condition of low-level southerly airflow which is to the east of Taihang Mountains in North China as well as the distribution of high emission areas in southern Hebei and northern Hubei (Fig. 1b); another high correlated zone which sits in Beijing-Tianjin and the Bohai Bay rim is possibly related to the weather condition of the more fog-haze "back-flow" of the easterly wind in North China. These analyses suggest that the North China PLAM/h and index features are significantly correlated to visibility, the high correlation area with significance level exceeding 0.001 is likely related to the regional distribution of meteorological condition of heavy fog weather in North China and the distribution of regional emission high-value zone in North China.

3.4 Application of PLAM/h index in fog-haze forecasting

3.4.1 The 20–26 February 2014 winter case analysis

Applying the PLAM/h index developed in this paper, 24 h forecasts of visibility with PLAM/h are conducted for one historically rarely-seen winter heavy fog-haze process in North China during the last half of February 2014 (20–26 February 2014). During the test, the NRT data of more than 670 stations in the North China region are adopted to analyze the correlation between PLAM/h index 24 h forecasts and visibility observation. Figure 6a and b reveal the correlation analysis results of PLAM/h index 24 h forecasts and observed visibility respectively at 08:00 (UTC +8), 20 February, and 08:00 (UTC +8) 22 February 2014. Table 1 lists the correlation of daily PLAM/h index 24 h forecasts and visibility during the whole process of the regional heavy fog-haze event over North China in 20–26 February 2014 as well as the number of stations that are involved in the test.

From Fig. 6 and Table 1 it can be seen the daily correlation coefficients (R^2) are 0.6529, 0.5424, 0.6047, 0.6040, 0.4550 and 0.3887, respectively; the significance levels all pass 0.001, which means their correlation is very good.

3.4.2 The 19–22 July 2013 summer case analysis

To further investigate the forecasting capability of summer PLAM/h index to the fog-haze area distribution, forecast application and testing analysis of one heavy fog-haze pollution process in North China in summer 19–22 July 2013 are carried out. On 19 July, extremely heavy fog emerged in the day time over Beijing, just as night had fallen. It was very dark with local visibility less than 5 m. Figure 7a and b reveal the correlation analysis result of PLAM/h index 24 h forecast and visibility during the polluting process in the North China region respectively at 08:00 (UTC +8) 20 and 22 July 2013. Table 2 presents the correlation of daily PLAM/h index 24 h forecast and visibility during the whole process of the regional heavy fog-haze event over North China in 19–22 July 2013 as well as the number of stations that participate in the forecasting test. From Fig. 7 and Table 2, the daily correlation coefficients (R^2) respectively are 0.4988, 0.4826, 0.5416 and 0.5263, and all their significance levels exceed 0.001.

The above analyses indicate that the PLAM/h index 24 h forecasts and visibility observations of the large-range samples in different winter and summer over North China all have higher correlations. This result illustrates the PLAM/h index would have good practical application prospect in forecasting the regional large-scale fog-haze weather in North China.

3.4.3 The 12 March 2014 fine weather case analysis

In order to investigate the analysis and identification capability of PLAM/h to the fine and sunny weather without fog or haze, the correlation between PLAM/h and visibility in a wide range of fine weather has been carried out. As an example, Fig. 8a and b reveal the correlation analysis of the regional PLAM/h distribution and PLAM/h index 24 h forecasts on 12 March 2014.

It is seen from Fig. 8a that most part of North China has low-value PLAM/h < 60 (blue area in the figure). The meteorological condition PLAM/h index distribution displays that large area of North China lies in the area with the meteorological condition extremely favorable for atmospheric dispersion. Beijing is under blue sky with clouds. The PLAM/h index forecasts of Beijing and Baoding (Hebei) are 53 and 29 respectively. From daytime to evening on 12 March, the $PM_{2.5}$ value of Beijing urban area is reported to be 21–35 $\mu g\,m^{-3}$.

Figure 8b is the correlation analysis of PLAM/h index 24 h forecasts and observed visibility at 677 stations in North China on 12 March 2014, which was made based on real-time data. It can be seen that the correlation coefficient (R^2) gets to 0.412 and the significance level passes 0.001 averagely. On 13 March 2014, Beijing continues to enjoy the clear weather with blue sky and clouds, so air quality is excellent. The $PM_{2.5}$ value of Beijing urban area still remains at high level of 22–37 $\mu g\,m^{-3}$. The above analysis indicates that for large-scale fine weather or low-visibility heavy pollution weather, PLAM/h index has the strong capability of identifying, analyzing and forecasting.

4 Conclusions

PLAM – a meteorological pollution index for air quality has been developed and used in NRT air quality forecasts, by considering both meteorology and pollutant emissions. Based on the emission diagnosing model of 2-dimensional probability density function, the paper has extended the parameterized description of original PLAM, applying it in the diagnosis and forecasting of the variation and distribution of wide-range regional low-visibility fog-haze intensity and achieving satisfactory results. The contrast analysis with or without the emission impact indicates that meteorological condition and emission factor jointly play the role in expanding PLAM towards high-value zone. This means that PLAM/h index involving emission has significant effect on improving the capability of diagnosing and forecasting heavy fog-haze weather in North China.

The variation of air quality meteorological condition index PLAM/h is significantly correlated to the regional visibility observations in North China. The correlation coefficients of wither, summer, spring and autumn are 0.8557 (winter), 0.8009 (summer), 0.7617 (spring) and 0.9552 (autumn), respectively and their average significance level goes beyond 0.001.

The correlation analysis of index and visibility regional distributions indicates that the high correlation zones respectively lie in Jing-Jin-Ji (Beijing, Tianjin, Hebei), Bohai Bay rim, southern Hebei and northern Hubei. This indicates that PLAM/h index is related to the distributions of the North China weather system and the heavy fog occurrence region as well as the distribution of emission high value zones, which is indicative to diagnose and identify the regional distribution of the fog-haze frequently, hit areas.

The analyses on typical high pollution cases of spring, summer, autumn and winter suggest that PLAM/h index regional distribution is related to the banding distribution features of weather-scale systems in different seasons. The weather-scale high-value PLAM/h areas correspond to the low-visibility areas, indicating the PLAM/h index has the diagnosing, identifying and forecasting capability to the wide-range fog-haze areas and their seasonal differences in North China.

Although winter is different from summer, the PLAM/h index 24 h forecasts and visibility observations from the weather stations of North China, including wide-range fine weather and the low-visibility heavy pollution weather, all have high correlations. This indicates the PLAM/h index has good identifying, analyzing and forecasting capabilities. These conclusions show that the PLAM/h index will have good practical application prospect in forecasting the large-scale fog-haze areas and their seasonal differences in North China.

Acknowledgements. This work was funded by the National Key Foundation Study Developing Programmers (2011CB403404, 2011CB403401), National Key Technology R&D Program (Grant no. 2014BAC16B01), National Natural Science Foundation of China under Grant (No. 41 275 167, No. 41 275 007).

References

Gong, S. L., Barrie, A., Blanchet, J. P., Salzen, K. N., Lohmann, U., Lesins, G., Spacek, L., Zhang, L. M., Girard, E., Lin, H., Leaitch, R., Leighton, H., Chylek, P., and Huang, P.: Canadian aerosol module: a size-segregated simulation of atmospheric aerosol processes for climate and air quality models 1. Module development, J. Geophys. Res., 108, 4007, doi:10.1029/2001JD002002, 2003.

Honoré, C., Rouil, L., and Vautard, R.: Predictability of European air quality: assessment of 3 years of operational forecasts and analyses by the PREV'AIR system, J. Geophys. Res., 113, D04301, doi:10.1029/2007JD008761, 2008.

Kassomenos, P., Papaloukas, C., Petrakis, M., and Karakitsios, S.: Assessment and prediction of short term hospital admissions: the case of Athens, Greece, Atmos. Environ., 42, 7078–7086, 2008.

Kuo, H. L.: Convective weather in conditionally unstable atmosphere, Tellus, 13, 441–459, 1961.

Kuo, H. L.: On formation and intensification of tropical cyclone through latent heat release in cumulus convection, J. Atmos. Sci., 22, 40–23, 1965.

Kuo, H. L.: Further studies on the parameterization of the influence of cumulus convection in large-scale flows, J. Atmos. Sci., 31, 1232–1240, 1974.

Li, Y., Wang, W., Wang, J. Z., Zhang, X. L., Lin, W. L., and Yang, Y. Q.: Impact of air pollution control measures and weather conditions on asthma during the 2008 Summer Olympic Games in Beijing, Int. J. Biometeorol., 55, 547–554, doi:10.1007/s00484-010-0373-6, 2011.

McKeen, S.: Evaluation of several real-time $PM_{2.5}$ forecast models using data collected during the ICARTT/NEAQS 2004 field study, J. Geophys. Res., 112, D10S20, doi:10.1029/2006JD007608, 2007.

Moran, M. D.: Particulate-matter forecasting with GEM-MACH15, a new Canadian operational air quality forecast model, in: Proceedings of the 30th NATO/SPS ITM on Air Pollution Modelling and Its Application, San Francisco, USA, 2009.

Neumann, C. J. and Mandal, G. S.: Statistical prediction of tropical storm motion over the Bay of Bengal and Arabian Sea, Indian J. Met. Geophys., 29, 487–500, 1978.

Rigby, M. and Toumi, R.: London air pollution climatology: indirect evidence for urban boundary layer height and wind speed enhancement, Atmos. Environ., 42, 4932–4947, 2008.

Wang, J. L. and Liu, X. L.: The discuss on relationship between visibility and mass concentration of $PM_{2.5}$ in Beijing, Acta Meteorol. Sin., 64, 221–228, 2006.

Wang, J. Z. and Neumann, C. J.: A Markov-type analogmedel for prediction of typhoon motion in Northwestern Pacific, Sci. Sinica, 28, 517–526, 1985.

Wang, J. Z., Xu, X. D., and Yang, Y. Q.: A study of characteristics of urban visibility and fog in Beijing and the surrouding area, Journal of Applied Meteorological Science Suppl., 13, 160–168, 2002 (in Chinese).

Wang, J. Z., Yang, Y. Q., Zhang, G. Z., and Yu, S. Q.: Climatic trend of cloud amount related to the aerosol characteristics in Beijing during 1950–2005, Acta Meteorol. Sin., 24, 762–775, 2010.

Wang, J. Z., Gong, S. L., Zhang, X. Y., Yang, Y. Q., Hou, Q., Zhou, C. H., and Wang, Y. Q.: A parameterized method for air-quality diagnosis and its applications, Adv. Meteorol., 2012, 238589, doi:10.1155/2012/238589, 2012.

Wang, J. Z., Wang, Y. Q., Liu, H., Yang, Y. Q., Zhang, X. Y., Li, Y., Zhang, Y. M., and Deng, G.: Diagnostic identification of the impact of meteorological conditions on $PM_{2.5}$ concentrations in Beijing, Atmos. Environ., 81, 158–165, 2013.

Yang, Y. Q., Wang, J. Z., Hou, Q., and Wang, Y. Q.: A Plam index for Beijing stabilized weather forecast in summer over Beijing, Journal of Applied Meteorological Science, 20, 649–655, 2009.

Title Page
Abstract Introduction
Conclusions References
Tables Figures
◀◀ ▶▶
◀ ▶
Back Close
Full Screen / Esc
Printer-friendly Version
Interactive Discussion

Zhang, X. Y., Wang, Y. Q., Lin, W. L., Zhang, Y. M., Zhang, X. C., Gong, S. L., Zhao, P., Yang, Y. Q., Wang, J. Z., hou, Q., Zhang, X. L., Che, H. Z., Guo, J. P., and Li, Y.: Changes of atmospheric composition and optical properties over Beijing 2008 Olympic Monitoring Campaign, B. Am. Meteorol. Soc., 90, 1633–1649, 2009.

Zhang, X. Y., Sun, J. Y., Wang, Y. Q., Li, W. J., Zhang, Q., Wang, W. Z., Qian, J. N.,Cao, G. L., Wang, J. Z., Yang, Y. Q., and Zhang, Y. M.: Factors contributing to haze and fog in China, Chin. Sci. Bull. (Chin. Ver.), 58, 1178–1187, doi:10.1360/972013-150, 2013 (in Chinese).

Table 1. Correlation of daily PLAM/h index 24 h forecasts and visibility during the whole process of the regional heavy fog-haze event over North China in 20–26 February 2014.

Forecast time	Correlaton coefficient (R^2)	Station number
08:00 20 Feb	0.6529	674
08:00 21 Feb	0.5424	668
08:00 22 Feb	0.4634	669
08:00 23 Feb	0.6047	676
08:00 24 Feb	0.6040	673
08:00 25 Feb	0.4550	678
08:00 26 Feb	0.3887	673

Table 2. Correlation of daily PLAM/h index 24 h forecasts and visibility during the whole process of the regional heavy fog-haze event over North China in 19–22 Jul 2013.

Forecast time	Correlaton coefficient (R^2)	Station number
08:00 19 Jul	0.4988	682
08:00 20 Jul	0.4826	683
08:00 21 Jul	0.5416	685
08:00 22 Jul	0.5263	181

Title Page
Abstract Introduction
Conclusions References
Tables Figures
◀ ▶
Back Close
Full Screen / Esc
Printer-friendly Version
Interactive Discussion

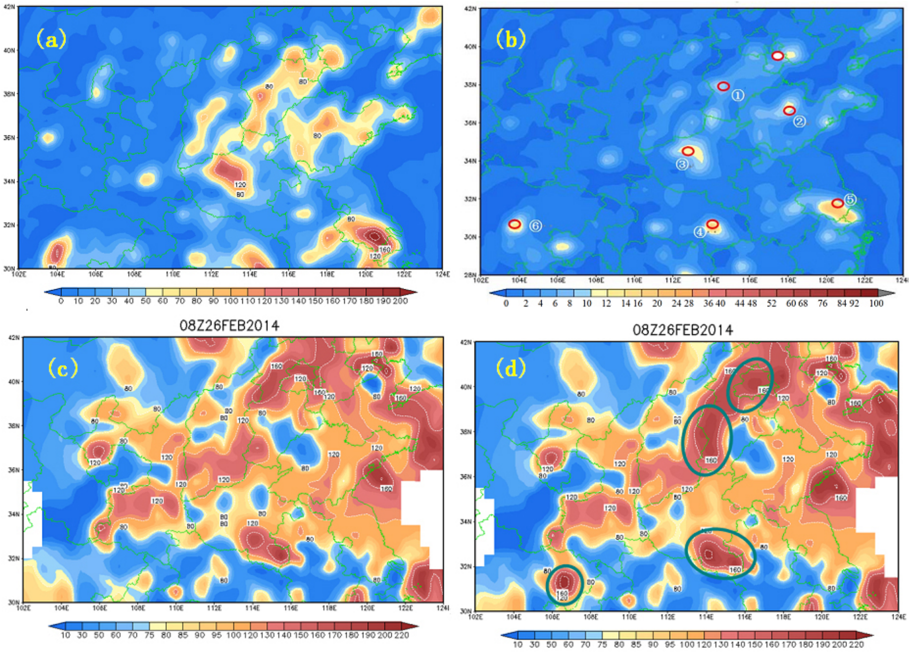

Figure 1. High resolution emission list E distribution **(a)** and its regional emission standardized list γ **(b)**; PLAM index distribution with ignoring **(c)** and considering **(d)** the emission condition in North China at 08:00 (UTC +8) 26 February 2014.

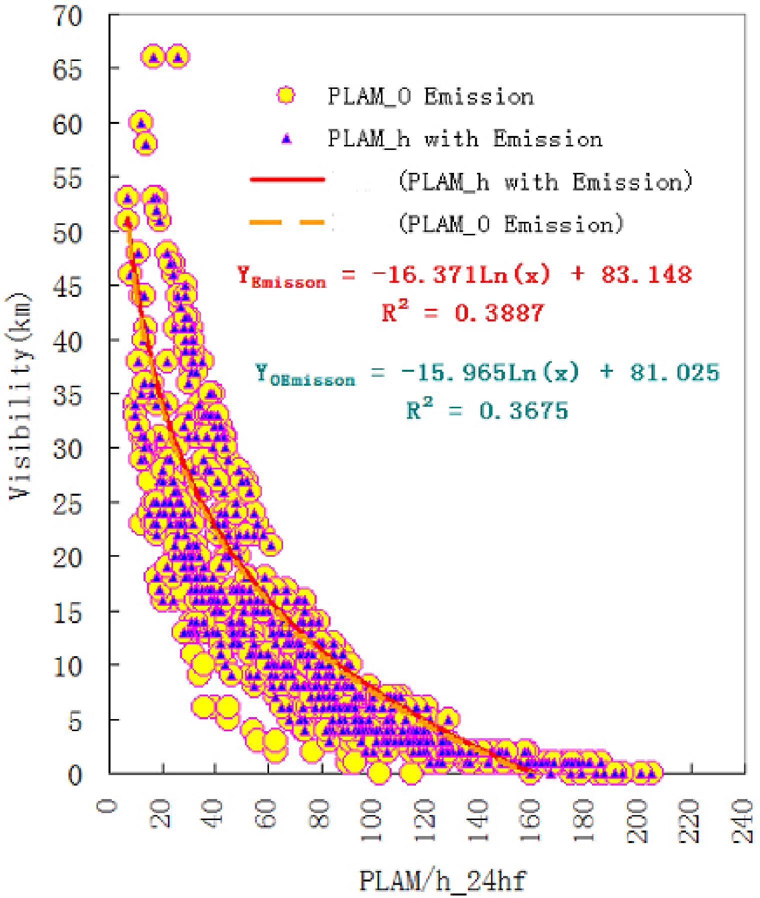

Figure 2. Correlation analysis of PLAM and visibility considering and not considering emission factors on 26 February 2014.

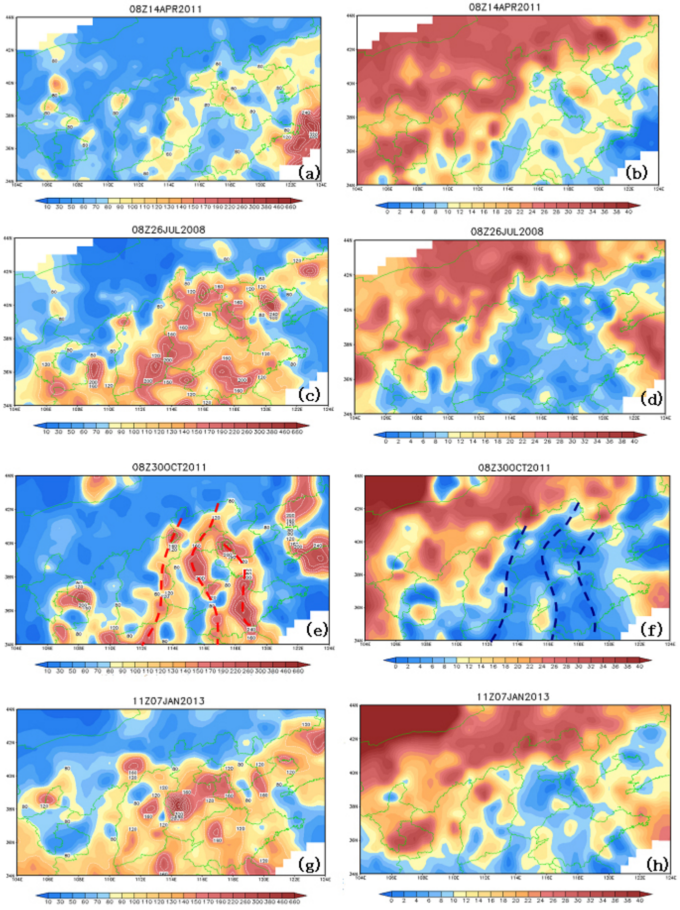

Figure 3. The cases for PLAM/h **(a)** and visibility **(b)** of the 14 April 2011 , PLAM/h **(c)** and visibility **(d)** of the 26 July 2008, PLAM/h **(e)** and visibility **(f)** of the 30 October 2011 and PLAM/h **(g)** and visibility **(h)** on 7 January 2011.

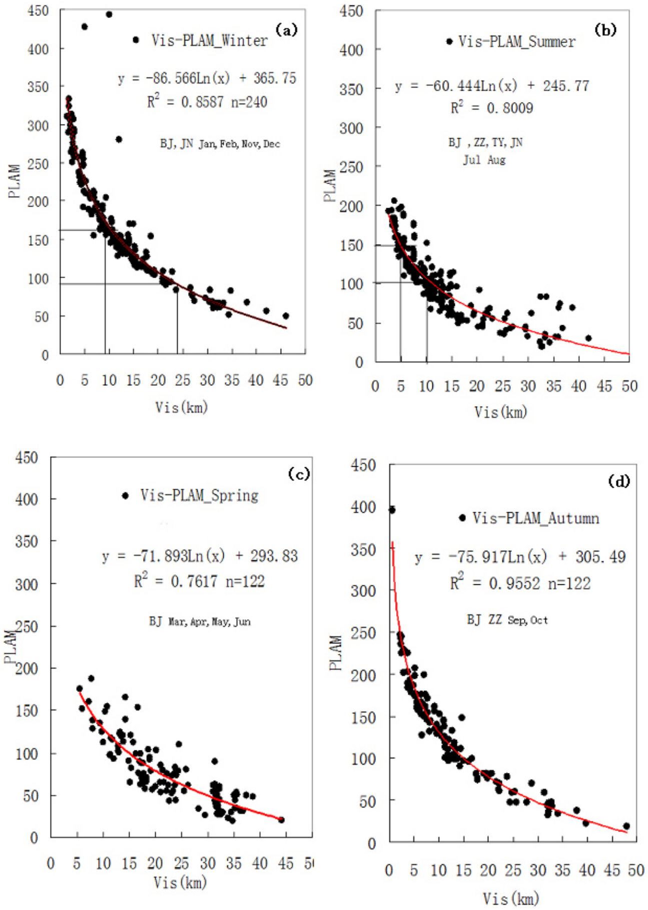

Figure 4. Correlation analysis of PLAM/h index and visibility in winter **(a)**, summer **(b)**, spring **(c)** and autumn **(d)**.

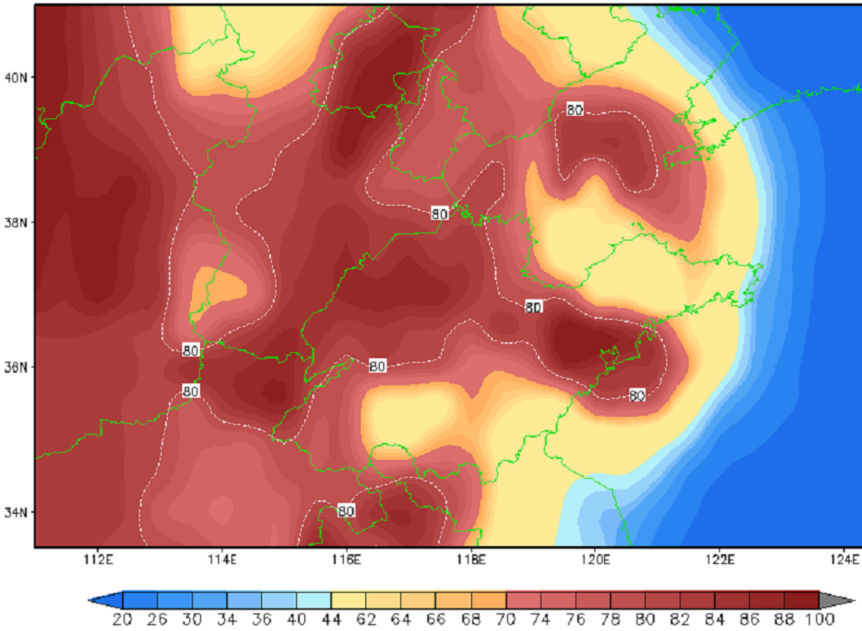

Figure 5. The regional correlation between PLAM/h index and visibility obtained by calculating the 1006 groups of observation samples collected from January 2009 to December 2012. The regional distribution of the correlation with significance level exceeding 0.001.

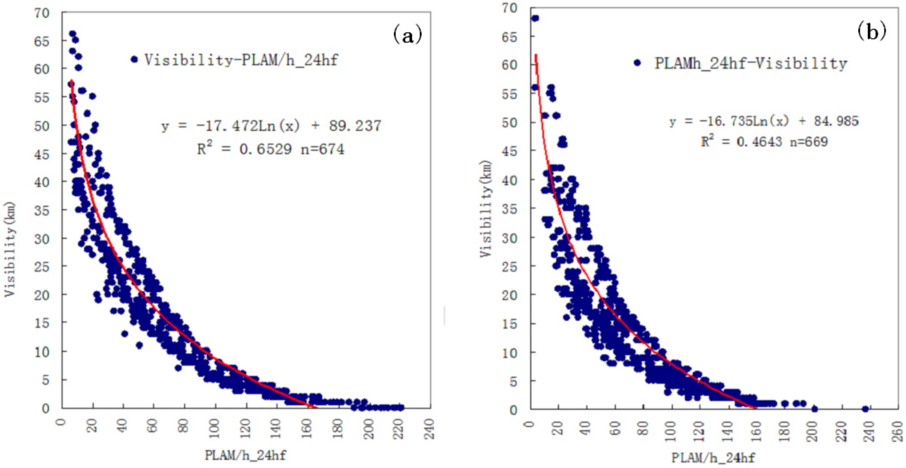

Figure 6. The correlation analysis results of PLAM/h index 24 h forecasts and observed visibility respectively at 08:00 (UTC +8) 20 **(a)** and 08:00 (UTC +8) 22 **(b)** February 2014.

ACPD
15, 9077–9106, 2015

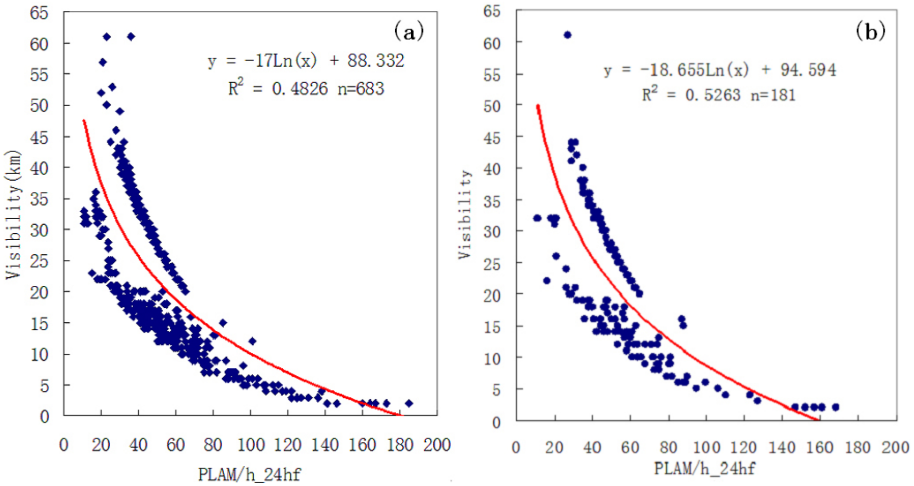

Figure 7. Correlation analysis of the regional PLAM/h index 24 h forecasts and visibility during the whole period of pollution in North China respectively at 08:00 (UTC +8) 20 **(a)** and 08:00 (UTC +8) 22 **(b)** July 2014.

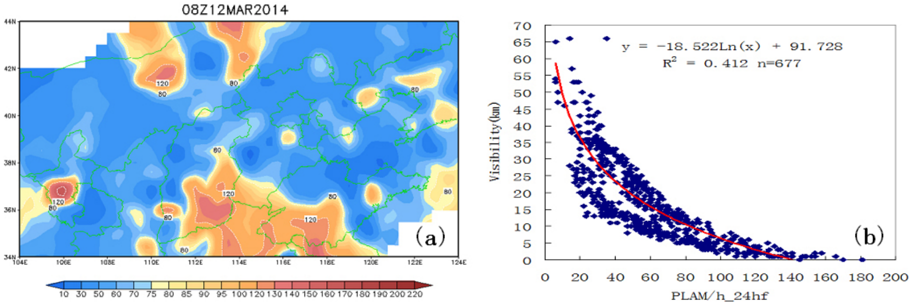

Figure 8. Distribution of PLAM/h in North China **(a)** and the correlation analysis of PLAM/h index 24 h forecasts and observed visibility in North China for 8:00 (UTC +8) 12 March 2014 **(b)**.

Title Page
Abstract | Introduction
Conclusions | References
Tables | Figures
◄| |►
◄ ►
Back | Close
Full Screen / Esc
Printer-friendly Version
Interactive Discussion